Pis'ma v ZhETF

# Transitions between "$\pi$" and "0" states in superconductor – ferromagnet – superconductor junctions.

*N. M. Chtchelkatchev*[1)],

*L. D. Landau Institute for Theoretical Physics RAS, 117940 Moscow, Russia*
*Institute for High Pressure Physics, Russian Academy of Sciences, Troitsk 142092, Moscow Region, Russia*
*Moscow Institute of Physics and Technology, Moscow 141700, Russia*

Submitted February 2, 2008

Experimental and theoretical study of superconductor (S) – ferromagnet (F) – superconductor junctions showed that in certain range of parameters (e.g., the length of the ferromagnet $d_F$, the exchange field, $E_{\rm ex}$) the ground state of a SFS junction corresponds to superconducting phase difference $\pi$ or 0. The phase diagram of a SFS junction with the respect to $\pi$ and 0 states is investigated in this letter in $E_{\rm ex}, d_F, T$ space. It is shown that the phase diagram is very sensitive to the geometry of the system, in particular, to the amount of disorder disorder.

PACS: 74.50.+r, 74.80.-g, 75.70.-i

Recently many interesting phenomena were investigated in Superconductor (S) - Ferromagnet (F) - Superconductor Josephson contacts. One of the most interesting effects is the so called $\pi$-state of SFS junctions [1–11] in which the equilibrium ground state is characterized by an intrinsic phase difference $\pi$ between the two superconductors.

Theoretical study of SFS junctions [1–3] showed that if $E_{\rm ex}$ is fixed in the ferromagnet then the $\pi$-state appears at $0 < d_F^{(1)} < d_F < d_F^{(2)}$, $d_F^{(2)} < d_F^{(3)} < d_F < d_F^{(4)}$ *etc...*, and near $d_F^{(i)}$ $(i = 1, 2, \dots)$ the critical current $I_c(d_F)$ has a cusp. Recent experiments [4, 5] showed that the critical current – temperature curve, $I_c(T)$, in SFS junctions at $d_F \approx d_F^{(i)}$, $i = 1, 2$ has also a cusp. The temperature of the cusp was identified with $\pi - 0$ transition temperature. These experiments became the motivation of the theoretical investigations of $I_c(T)$ curves and phase diagrams of SFS junctions. It was shown in Refs. [8, 9] that if $d_F \approx d_F^{(i)}$ $(i = 1, 2, \dots)$ in very short *ballistic* SFS junctions ($d_F \ll \xi_0 = \hbar v_F/\Delta(T = 0)$) then there is $\pi - 0$ transition at certain temperature and the $\pi$ state is always (for all $i$) at larger temperatures then 0-state. This prediction is in contradiction with the experimental data and calculations of the phase diagram in dirty SFS junctions based on linearized Usadel equations, see Ref. [5] and Refs. there in, where the order of $\pi$ and 0 phases with the respect to the temperature is one at $d_F \approx d_F^{(1)}$ and the opposite at $d_F \approx d_F^{(2)}$. SFS junctions investigated in Ref. [5] were dirty. From the first glance it may seem that disorder strongly influences on the phase diagram of SFS junctions. This is exactly so. It is shown in this letter that the phase diagram of SFS junctions is rather sensitive the geometry of the system, in particular, to the amount of disorder in the junction.

The paper is organized as follows: most of the paper is devoted to investigations of phase diagrams of SFS junctions near the first cusp of $I_c(d_F)$ (at $d_F \approx d_F^{(1)}$), and the case $d_F \approx d_F^{(i)}$, $i > 1$ is discussed in end.

The superconducting SFS junction that is investigated here is sketched in Fig.1. A barrier (e.g., an insulator layer) is situated at position $x = a$ from the junction center.

First will be considered ballistic SFS junctions. I assume that the exchange energy of the ferromagnet $E_{\rm ex} \ll E_F$; there is no barrier at SF boundaries: the probability of Andreev reflection of subgapped Bogoliubov quasiparticles from a SF boundary is equal to unity; variation of the superconducting gap in S near the boundary will be neglected (this is correct approximation if our SFS is a quantum point contact [12,13]; in other cases this approximation can be used because it usually leads only to few percent mistakes in the Josephson current). Then the Josephson current can be found, for instance, using scattering matrix method [8, 12]:

$$I(\varphi) = \frac{2e}{\hbar}\frac{1}{2}\sum_{\sigma=\pm 1} T \sum_{\omega} \partial_\varphi \ln g(\omega, \varphi, \sigma), \qquad (1)$$

where

$$g(\omega, \varphi, \sigma) = (2\omega^2 + \Delta^2)\cosh(\Phi) + \\ + 2\omega\sqrt{\omega^2 + \Delta^2}\sinh(\Phi) + \mathcal{T}\cos\varphi + \mathcal{R}\cosh\beta. \qquad (2)$$

Here $\varphi$ is the phase difference between the superconductors; $\Delta$ is the bulk superconducting gap; $\omega = 2\pi(n +$

[1)]e-mail: nms@itp.ac.ru

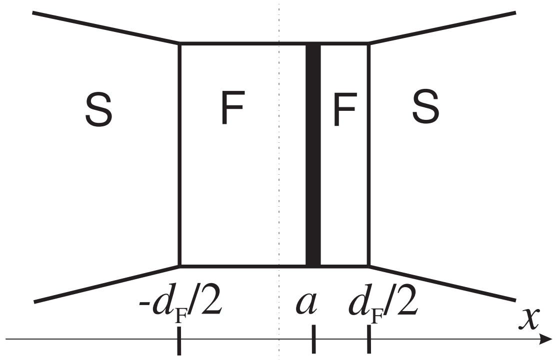


Fig.1. A sketch of a SFS junction. A barrier (e.g., an insulator layer) is situated at position $x = a$ from the junction center.

$1/2)$, $n = 0, \pm 1, \ldots$; $\Phi = 2d_F(\omega + iE_{\rm ex}\sigma)/\hbar v_F \cos\theta$, $\beta = 4a(\omega + iE_{\rm ex}\sigma)/\hbar v_F \cos\theta$ and $\mathcal{T} = t_\uparrow t_\downarrow$, $\mathcal{R} = r_\uparrow r_\downarrow$, where $(t_\uparrow)^2$, $(r_\uparrow)^2$ are transmission and reflection probabilities of the barrier for spin-up electrons, and $\theta$ is the angle between the trajectory and the $X$-axis. Eqs.(1)-(2) can be generalized if the ratio $E_{\rm ex}/E_F$ is arbitrary. Then, for example, $\Phi = {\rm Im}\, d_F\{\sqrt{2m(E_F + i\omega + E_{\rm ex}\sigma)} - \sqrt{2m(E_F - i\omega - E_{\rm ex}\sigma)}\}$, $\beta$ can be written in a similar way. $\omega$-dependence of $\Phi$ was neglected in Refs. [7–9] because there $d_F$ was much smaller then $\xi_0$. Physically ballistic model of a SFS junction could be realized, for example, in gated heterostructures [14] or in the break-junctions [15] in external magnetic field producing Zeeman splitting of Andreev levels. [16]

The case $a = 0$ (then the scattering potential of the junction is symmetric), $d_F \lesssim \xi = \hbar v_F/\Delta$ was considered in the papers [7–9]. This model is important because on qualitative level it well describes SFS junctions where F is a ferromagnetic granule or a spin-active interface, see Ref. [7] and refs. therein. It was shown that if one fixes $E_{\rm ex}$ and changes the temperature then the $\pi$-state of a ballistic SFS junction appears usually at higher temperatures then 0-state. This is not so if the junction is dirty and there is no other scattering potential in the junction then the impurity potential. To illustrate this point of view i consider Josephson current in two similar SFS junctions with the same dimensionless normal conductance per channel, same $\Delta$, $E_{\rm ex}$, number of open channels, etc... The only difference between the junctions that in the first one the normal conductance is provided by an insulator layer with a flat surface at the center of the ferromagnet like in Fig.1 and in the second one — by nonmagnetic impurities in the ferromagnetic region. Following parameters were chosen: $d_F = \xi_0 = \hbar v_F/\Delta_0$, $\Delta_0 = \Delta(T = 0)$; $\Theta = 2d_F E_{\rm ex}/\pi\xi_0\Delta_0 = 0.18$. The disorder strength in the second junction was $\Delta_0/\tau = 10$,

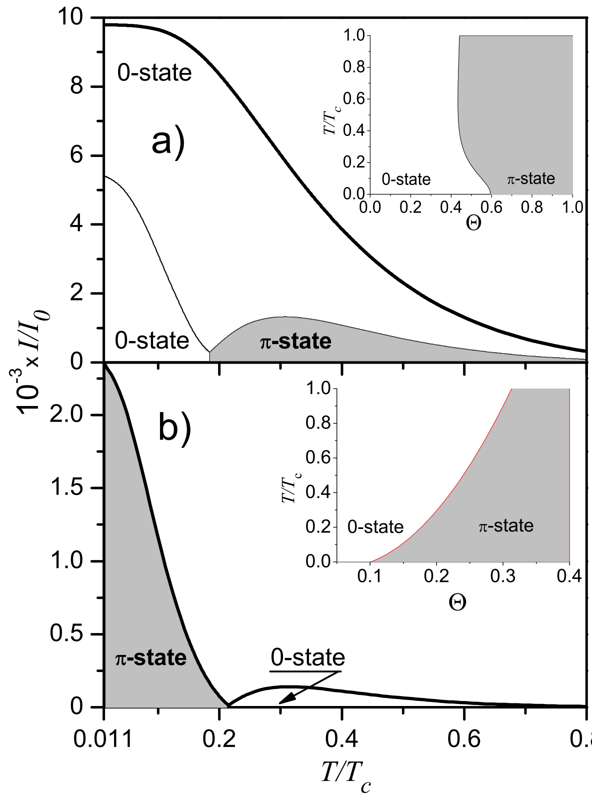


Fig.2. The figures show critical current – temperature relations in two short SFS junctions with the same normal conductance, near the first minimum of $I_c(d_F)$ (at $d_F \approx d_F^{(1)}$). Fig.2a corresponds to ballistic junction and Fig.2b — to dirty one. The insets show "phase diagrams" of the junctions. The current scale $I_0 = N_{\rm ch} e\Delta_0/\hbar$, where $N_{\rm ch}$ is the number of open channels in the junction. The thick curve in Fig.2a corresponds to the same $\Theta = 0.18$ as in Fig.1b; the other curve in Fig.2a corresponds to $\Theta \approx 0.5$. It is seen that the $\pi$-state in a ballistic SFS junction is at higher temperatures then 0-state; the opposite phenomenon takes place in a dirty SFS junction.

where $\tau v_F$ is the mean free path. The transmission probability of the insulator layer in the first junction was $D(\theta) = D_0 \cos^2\theta/(1 - D_0 + D_0\cos^2\theta)$, with $D_0 = 0.127$. The current scale $I_0 = N_{\rm ch} e\Delta_0/\hbar$, where $N_{\rm ch}$ is the number of open channels in the junction. The thick curve in Fig.2a corresponds to the same $\Theta = 0.18$ as in Fig.1b; the other curve in Fig.2a corresponds to $\Theta \approx 0.5$. It follows that near the first cusp of $I_c(d_F)$ (i.e., $d_F \sim d_F^{(1)}$) $\pi$-state in a short ballistic SFS junction is at higher temperatury then 0-state; the opposite phenomenon takes place in a dirty SFS junction. If there is an insulator barrier in a ballistic short SFS junction and we add nonmagnetic impurities in it then the transition from the case shown in Fig.2a to the case shown

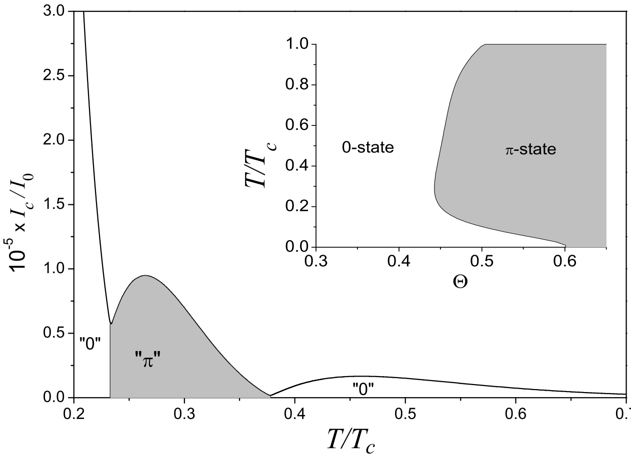


Fig.3.The figure exhibits critical current – temperature relation in a long $d_f \approx 3\xi_0$ ballistic SFS junction with $D_0 = 0.127$, $\Theta \approx 0.445$, near the first minimum of $I_c(d_F)$ (at $d_F \approx d_F^{(1)}$). The inset shows the "phase diagram" of the junction. If impurities were added in this type of junctions then the phase diagram would finally look like in Fig.2b. If i make $D_0 \approx 1$, see Fig.4, then the phase diagram will become similar to the phase diagram shown in Fig.2b.

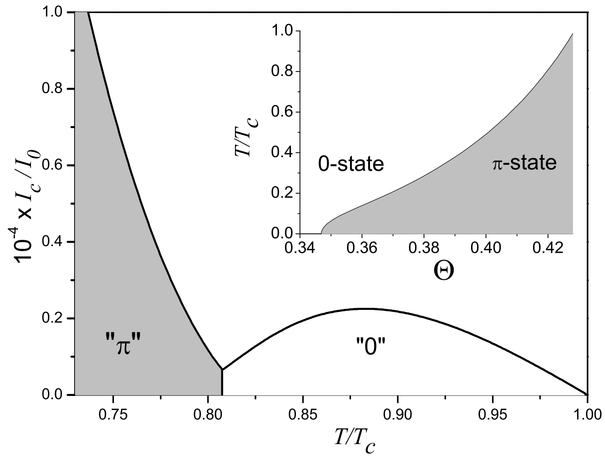


Fig.4. The figure shows critical current – temperature relation in a long $d_f \approx 3\xi_0$ *ballistic* SFS junction with $D_0 = 1$, $\Theta \approx 0.42$, near the first minimum of $I_c(d_F)$ (at $d_F \approx d_F^{(1)}$). The inset shows the "phase diagram" of the junction. The phase diagram (and the current temperature relation) in a short dirty SFS junction, Fig.2b, looks quite similar to one shown in Fig.5.

in Fig.2b is expected to occur when $l/d_F \sim D$, where $l$ is a mean free path. Josephson current calculations in ballistic junctions were performed using Eqs.(1)-(2) with $t_\uparrow = t_\downarrow = \sqrt{D}$, in dirty junctions — using Ricatti form of Eilenberger quasiclassical equations [17].

A "short" SFS junction with $d_F \lesssim \xi_0$ was considered above. What may happen if $d_F > \xi_0$ is illustrated in Fig.3. The junction is ballistic (with the same normal conductance corresponding to $D_0 = 0.127$) and $d_F \approx 3\xi_0$. The inset shows the "phase diagram" of the junction. So by freezing long SFS junction (at $d_F \approx d_F^{(1)}$) starting from $T_c$ one can go through a sequence of phase transitions: $0 \to \pi \to 0$. In general one can make junction phase diagram similar to any phase diagram depicted in Figs.1-3 by the proper choice of the position of the insulator barrier and the length of the junction. For example, if i make $D_0 = 1$ then the phase diagram in Fig.1 will transform to the phase diagram shown in Fig.2b (the junction is ballistic!). This is shown in Fig.4. The same transformation of the phase diagram occurs due to impurities as show numerical calculations.

Below is given a short description of numerical calculation procedure that was used for drawing of Fig.2b. Calculations were done using Ricatti representation of the Eilenberger quasiclassical equations (because Eilenberger equations are unstable) [17]. The quasiclassical Green functions can be parameterized via the new functions $a$ and $b$, so

$$f = \frac{2a}{1+ab}\,\mathrm{sign}\,\omega, \qquad g = \frac{1-ab}{1+ab}\,\mathrm{sign}\,\omega. \tag{3}$$

The amplitudes $a, b$ change according to the Ricatti equations

$$\begin{aligned} \mathbf{v}_F\nabla a + 2\omega_R a + \tilde{\Delta}_R a^2 - \Delta_R = 0, \\ \mathbf{v}_F\nabla b - 2\omega_R b - \Delta_R b^2 + \tilde{\Delta}_R = 0, \end{aligned} \tag{4}$$

where $\Delta_R = \Delta + \frac{\langle f\rangle}{2\tau}$, $\tilde{\Delta}_R = \Delta^* + \frac{\langle \tilde{f}\rangle}{2\tau}$ and $\omega_R = \omega_n + i\sigma E_{\rm ex} + \langle g\rangle/2\tau$. Here $\langle\ldots\rangle$ denotes averaging over directions of the quasiclassical trajectories, $\tau$ is the mean free path of an electron in the impurity potential. Eqs.(4) were solved numerically self consistently, the Josephson current density was evaluated as follows:

$$j = -i\pi e\nu T\sum_\omega\sum_\sigma \langle \mathbf{v}_F g\rangle_{\mathbf{v}_F}, \tag{5}$$

where $\nu$ is the normal density of states. I tried to expand the Ricatti equations over $\tau^{-1}$ in the first order to find analytically how disorder influences on the phase diagram of a short SFS junction. Calculations showed no effect in the first order.

The discussion above may lead to a conclusion that in *dirty* Josephson junctions with ferromagnet layers between superconductors the phase diagram always looks similar like in Fig.2b if $d_F \sim d_F^{(1)}$. It seems that this

statement is true for short SFS junctions, but this is not true in general. To prove it i shall give below an example (more examples and detailed discussion will be give in the extended version of this letter). Consider a dirty SFIFS junction (e.g., like in Fig.1a). The Josephson current can be found from Usadel equations [17]. In general Usadel equations are nonlinear over quasiclassical greens functions. But near the critical temperature of the junction or if superconductors and ferromagnets are weakly coupled the Usadel equations can be linearized. Then the linearized Usadel equations in the ferromagnets for anomalous function $f$ look like:

$$\partial^2 f - \frac{2|\omega| + 2iJ_{1,2}\sigma \operatorname{sign}\omega}{D_{1,2}} f = 0, \tag{6}$$

where $D_{1,2}$ is the diffusion constant and $J_{1,2}$ — the exchange energy in the left (right) ferromagnetic layer. If the magnetizations of the ferromagnetic layers are collinear then the $f$-function to the left of the insulator layer I, see Fig.1b, is $f = \frac{1}{\sqrt{|\kappa_1/\rho_1|}}(Ae^{\kappa_1 x} + Be^{-\kappa_1 x})$ and to the left — $f = \frac{1}{\sqrt{|\kappa_2/\rho_2|}}(Ce^{\kappa_2 x} + De^{-\kappa_2 x})$. Here $\kappa_{1,2} = \sqrt{(|\omega| + 2iJ_{1,2}\sigma \operatorname{sign}\omega)/D_{1,2}}$, where $\rho_{1,2}$ is the resistivity of the ferromagnets. The amplitudes $A, B, \ldots$ are not independent but they are connected by boundary conditions [18] that I write here in the matrix form:

$$\begin{pmatrix} B \\ C \end{pmatrix} = S \begin{pmatrix} A \\ D \end{pmatrix}, \tag{7}$$

$$S = \begin{pmatrix} e^{2\kappa_1 a}\frac{\tilde\kappa_1 - \tilde\kappa_2 - \tilde\kappa_1\tilde\kappa_2 R}{\tilde\kappa_1 + \tilde\kappa_2 - \tilde\kappa_1\tilde\kappa_2 R} & e^{(\kappa_1-\kappa_2)a}\frac{\sqrt{\tilde\kappa_1\tilde\kappa_2}}{\tilde\kappa_1 + \tilde\kappa_2 - \tilde\kappa_1\tilde\kappa_2 R} \\ e^{(\kappa_1-\kappa_2)a}\frac{\sqrt{\tilde\kappa_1\tilde\kappa_2}}{\tilde\kappa_2 + \tilde\kappa_1 - \tilde\kappa_1\tilde\kappa_2 R} & e^{-2\kappa_2 a}\frac{\tilde\kappa_2 - \tilde\kappa_1 - \tilde\kappa_1\tilde\kappa_2 R}{\tilde\kappa_2 + \tilde\kappa_1 - \tilde\kappa_1\tilde\kappa_2 R} \end{pmatrix}, \tag{8}$$

where $S$ is the "scattering matrix" of the F-F boundary (diagonal elements of $S$ play the role of "reflection" amplitudes, off diagonal — "transmission" amplitudes). Here $\tilde\kappa_{1,2} = \kappa_{1,2}/\rho_{1,2}$; $R$ is resistance of the F-F boundary. When $R = 0$, the scattering matrix $S$ is similar to the quantum mechanical scattering matrix of a potential step. At the SF interface the boundary conditions look like:

$$\begin{pmatrix} A \\ D \end{pmatrix} = S_b \begin{pmatrix} B \\ C \end{pmatrix} - \vec\Delta_{\text{eff}}, \tag{9}$$

$$S_b = \begin{pmatrix} e^{2\kappa_1 d_F} & 0 \\ 0 & e^{2\kappa_2 d_F} \end{pmatrix}, \tag{10}$$

$$\vec\Delta_{\text{eff}} = \begin{pmatrix} \frac{\Delta_L e^{\kappa_1 d_F}}{\Omega R_L} \\ \frac{\Delta_R e^{\kappa_2 d_F}}{\Omega R_r} \end{pmatrix}, \tag{11}$$

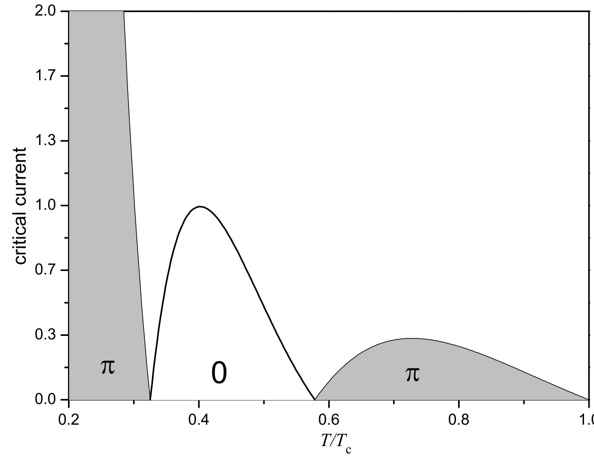


Fig.5. The figure shows critical current – temperature dependence in the dirty SFIF'S junction with parameters: $J_1 = -1.9T_c$, $J_2 = 3T_c$, $d_F/\xi = 1$, $a/\xi = -0.2$, $D_1 = D_2$, ($\xi = \sqrt{D/T_c}$), $R/(\rho_1\xi) = 0.1$. Here $d_F$ is again near $d_F^{(1)}$. The critical current is normalized on its value in the maximum of $I_c(T)$ corresponding to 0-state.

where $\Delta_{L(R)} = \Delta\exp(\pm i\phi/2)$ are the gaps of the left (right) superconductors, $\Omega = \sqrt{|\Delta|^2 + \omega^2}$, $R_{L(r)}$ are the resistances of the SF boundaries. From Eqs.(7)-(11) i get:

$$\begin{pmatrix} A \\ D \end{pmatrix} = (S_b S - 1)^{-1}\vec\Delta_{\text{eff}}. \tag{12}$$

The approach applied above is similar with the scattering matrix method used in Ref. [12] for calculation of the Josephson current in SNS junctions. Then the Josephson current density can be found: $j = \frac{\sigma_N \pi i}{2e} T\sum_\omega \operatorname{Tr}\{\tilde f \partial f - f\partial\tilde f\}$, where Tr is taken over spin degrees of freedom and $\tilde f(\omega) = f^*(-\omega)$. Fig.5 shows critical current – temperature dependence in the dirty SFIF'S junction with parameters: $J_1 = -1.9T_c$, $J_2 = 3T_c$, $d_F/\xi = 1$, $a/\xi = -0.2$, $D_1 = D_2$, ($\xi = \sqrt{D/T_c}$), $R/(\rho_1\xi) = 0.1$. Linearization of the Usadel equations is correct at these parameters. Fig.5 is similar to Fig.3 corresponding to ballistic SFS junction.

The phase diagrams were considered above in $(T, \Theta) \sim (T, E_{\text{ex}})$ space at fixed $d_F$. If one fixes $E_{\text{ex}}$ near the first cusp of $I_c(E_{\text{ex}})$ and changes $d_F$ he will obtain similar figures.

Everywhere above I considered phase diagrams of SFS junctions near the first cusp of $I_c(d_F)$ (at $d_F \approx d_F^{(1)}$). Below I briefly discuss the phase diagram in general case. Fig.6 shows tree phase diagrams. In all the figures $2E_{\text{ex}}/\pi\Delta_0 = 1$. The first and the second diagrams, Figs.6(a-b), correspond to ballistic SFS junc-

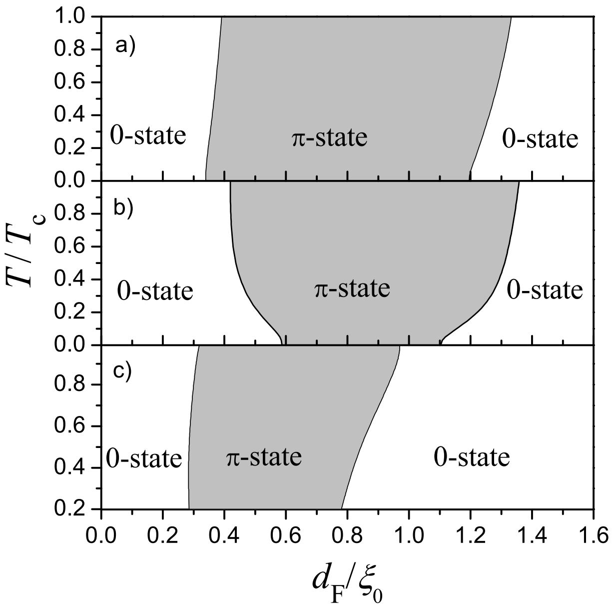


Fig.6. This figure illustrates how geometry of a SFS junction and disorder could influence on the shape of the phase diagram. In all figures $2E_{ex}/\pi\Delta_0 = 1$. The first and the second diagrams, Figs.6(a-b), correspond to ballistic SFS junctions described by Eqs.(1)-(2) with $D_0 = 1$ (no layer I, see Fig.1) and $D_0 = 0.127$, $a = 0$ correspondingly. The role of impurities can be seen in Fig.6(c). There $D_0 = 1$ and $\hbar/(\Delta_0\tau) = 10$. At $d_F/\xi_0 = 1$ the normal conductance of the junction in Fig.6(c) becomes equal to the normal conductance of the junction shown in Fig.6(a). If I draw the phase diagrams for the SFS junctions in $\Theta, T_c$ space it will look similar to Fig.6.

tions described by Eqs.(1)-(2) with $D_0 = 1$ (no layer I, see Fig.1) and $D_0 = 0.127$ correspondingly. The role of impurities can be seen in Fig.6(c). There $D_0 = 1$ and $\hbar/(\Delta_0\tau) = 10$. At $d_F/\xi_0 = 1$ the normal conductance of the junction in Fig.6(c) becomes equal to the normal conductance of the junction shown in Fig.6(a). If I'd use the linearized Usadel equations to describe the phase diagram of a SFS junction then I'd get the graph like in Fig.6(c). The phase diagram in Fig.6(c) qualitatively agrees with experimental results in Ref. [5] that the order of $\pi$ and 0 phases with the respect to the temperature is one at $d_F \approx d_F^{(1)}$ and the opposite at $d_F \approx d_F^{(2)}$.

In conclusion, $\pi - 0$ transitions in Josephson junctions with ferromagnetic layers are investigated in this letter. It is shown that the phase diagram is very sensitive to the geometry of the system, in particular, to the amount of disorder in the junction.

I'm grateful to I.S. Burmistrov, A.S. Iosselevich and especially Yu.S. Barash for stimulating discussions. I also thank RFBR Project No. 03-02-16677 and No 02-02-16622, the Russian Ministry of Science, the Netherlands Organization for Scientific Research NWO, CRDF, Russian Science Support foundation and State Scientist Support foundation (Project No. 4611.2004.2).

1. L. N. Bulaevskii, V. V. Kuzii, and A. A. Sobyanin, Pis'ma Zh. Eksp. Teor. Fiz. **25**, 314 (1977) [JETP Lett. **25**, 290 (1977)].
2. A. V. Andreev, A. I. Buzdin, and R. M. Osgood, Phys. Rev. B **43**, 10124 (1991).
3. A. I. Buzdin, B. Vujicic, and M. Yu. Kupriyanov, Zh. Eksp. Teor. Fiz. **101**, 231 (1992) [Sov. Phys. JETP **74**, 124 (1992)].
4. A. V. Veretennikov, V. V. Ryazanov, V. A. Oboznov *et al.*, Physica B **284-288**, 495 (2000); V. V. Ryazanov, V. A. Oboznov, A. Yu. Rusanov *et al.*, Phys. Rev. Lett. **86**, 2427 (2001).
5. V. V. Ryazanov, V. A. Oboznov, A.S. Prokofiev *et al*, J. Of Low Temp. Phys. **136**, 385 (2004).
6. T. Kontos, M. Aprili, J. Lesueur, *et al*, Phys. Rev. Lett. **89**, 137007 (2002)
7. M. Fogelström, Phys. Rev. B **62**, 11812 (2000).
8. N. M. Chtchelkatchev, W. Belzig, Yu. V. Nazarov, and C. Bruder, JETP Lett., **74**, 323 (2001) [Pisma v Zh. Eksp. i Teor. Fiz., Vol. 74, No. 6, 2001, pp. 357361].
9. Yu. S. Barash and I. V. Bobkova, Phys. Rev. B **65**, 144502 (2002).
10. Z. Radovic, N. Lazarides, and N. Flytzanis, Phys. Rev. B **68**, 014501 (2003).
11. A.A. Golubov, M.Yu. Kupriyanov, and Ya.V. Fominov, Pis'maZh. Eksp. Teor. Fiz. **75**, 223 (2002) [JETP Lett. **75**, 190 (2002)].
12. C.W.J. Beenakker, Phys. Rev. Lett. **67**, 3836 (1991).
13. A. Furusaki, H. Takayanagi, and M. Tsukada, Phys. Rev. Lett. **67**, 132 (1991) and Phys. Rev. B **45**, 10563 (1992).
14. H. Takayanagi, T. Akazaki, and J. Nitta, Phys. Rev. Lett. **75**, 3533 (1995).
15. E. Scheer, N. Agrait, J.C. Cuevas, A.L. Yeyati, B. Ludoph, A. Martin-Rodero, G.R. Bollinger, J.M. van Ruitenbeek, and C. Urbina, Nature **394**, 154 (1998).
16. S.K. Yip, Phys. Rev. B **62**, R6127 (2000).
17. W. Belzig, F. K. Wilhelm, C. Bruder *et al.*, Superlattices and Microst. **25**, 1251 (1999).
18. M. Yu. Kupriyanov and V. F. Lukichev, Zh. Exp. Teor. Fiz. **94**, 139 (1988) [Sov. Phys. JETP **67**, 1163 (1988)].